The Journal of Neuroscience, May 1995, 15(5): 3390–3399

Exocytosis in Peptidergic Nerve Terminals Exhibits Two Calcium-Sensitive Phases during Pulsatile Calcium Entry

Elizabeth P. Seward,[a] Natalya I. Chernevskaya, and Martha C. Nowycky

Department of Anatomy and Neurobiology, Medical College of Pennsylvania, Philadelphia, Pennsylvania 19129

The link between electrical activity, Ca^{2+} entry through voltage-gated channels, and transmitter or hormone secretion is a central issue in neurobiology. In peptidergic nerve terminals of the mammalian neurohypophysis (NHP), secretion is elicited by patterned bursts of action potentials (APs). All parameters of the bursts are important to elicit efficient secretion, including AP frequency, AP broadening, burst duration, and interburst interval (Leng, 1988).

We have studied Ca^{2+}-secretion coupling of peptide-containing large dense-core vesicles (LDCV) in isolated rat NHP terminals. Ca^{2+} influx through voltage-gated Ca^{2+} channels was elicited and recorded by the whole-cell patch-clamp technique. Exocytosis was monitored on line with high temporal resolution by the capacitance detection technique (Neher and Marty, 1982). AP bursts were simulated by depolarizing pulse trains that mimic pulsatile submembrane Ca^{2+} elevations predicted for physiological stimuli.

The characteristic capacitance response (ΔC_m) to a train of depolarizing pulses was triphasic. It consisted of a threshold phase during which early pulses did not elicit secretion, a subsequent secretory phase during which C_m increases were coupled to depolarizing pulses, and a fatigued or inactivated state during which additional Ca^{2+} entry was ineffective. Both the threshold phase and secretory phase were correlated with the integrals of Ca^{2+} current. Ca^{2+} chelators affect both the threshold and secretory phase at submillimolar concentrations. Thus, a "shell" rather than "microdomain" model of Ca^{2+} elevation is appropriate for analyzing Ca^{2+}–secretion coupling in NHP terminals (Nowycky and Pinter, 1993). We propose a two-step model, with a Ca^{2+}-dependent preparatory step followed by a final exocytotic step that is coupled to active Ca^{2+} influx.

The results suggest that under physiological conditions, APs early in a burst prepare an NHP terminal for secretion, but later APs actually trigger exocytosis. Since NHP terminals do not possess a readily releasable pool of vesicles that require only a single Ca^{2+} step for exocytosis as seen in chromaffin cells (Neher and Zucker, 1993) and melanotrophs (Thomas et al., 1993a), Ca^{2+}–secretion coupling mechanisms may be heterologous even within a single class of vesicles.

[Key words: exocytosis, peptide secretion, large dense-core vesicles, capacitance measurements, neurohypophysis]

At fast synapses, classical neurotransmitters are stored in small clear synaptic vesicles (SSVs) that are released extremely rapidly and are tightly coupled to pathways for Ca^{2+} influx (Augustine et al., 1987). Peptide transmitters and hormones are packaged in a second class of exocytotic vesicle or granule collectively called large dense-core vesicles (LDCVs). These differ from SSVs in structure and composition, and in many steps of their life cycle including synthesis, transport, release, and recycling mechanisms (reviewed in DeCamilli and Jahn, 1990). In contrast to SSVs, they are not localized to specialized structures such as active zones, but appear more widely dispersed at nerve terminals and dendrites of neurons (Zhu et al., 1986; Morris and Pow, 1988). The Ca^{2+} coupling of LDCV secretion also differs from that of SSV. In preparations where SSVs and LDCVs coexist, a localized submembrane increase of $[Ca^{2+}]$ is much more effective at evoking release of SSVs, while uniform elevation of Ca^{2+} favors predominantly LDCV release (Burgoyne, 1991; Verhage et al., 1991).

Until recently, due to technical limitations, Ca^{2+}–stimulation coupling of LDCVs has been studied mostly in populations of intact or permeabilized cells (Burgoyne, 1991). The membrane capacitance (C_m) detection technique, executed in whole-cell patch-clamp mode, permits investigation of Ca^{2+}–secretion coupling of LDCVs in single cells with a temporal resolution in the millisecond range and a sensitivity that detects the fusion of a few LDCVs (Neher and Marty, 1982). Using this technique, models of Ca^{2+}–secretion coupling of LDCVs have been proposed for chromaffin cells (Augustine and Neher, 1992; Heinemann et al., 1993; Neher and Zucker, 1993) and melanotrophs (Thomas et al., 1993a,b). In both models, a small population of docked (Thomas et al., 1993a) or readily releasable (Heinemann et al., 1993) LDCVs is available at rest and is exocytosed rapidly (~1000 fF/sec) as a third- or higher-order power of $[Ca^{2+}]$ elevation. On depletion, this pool is refilled slowly by a mechanism that is sensitive to Ca^{2+} and has a maximal rate of 45 fF/sec in chromaffin cells (Heinemann et al., 1993) or 26 fF/sec in melanotrophs (Thomas et al., 1993a).

We have investigated the applicability of these models to isolated neurohypophysial (NHP) nerve terminals, a classical preparation for the study of Ca^{2+}-stimulated peptide release (Douglas and Poisner, 1964a,b; Cazalis et al., 1987a,b; Leng, 1988). NHP terminals secrete the peptide hormones oxytocin and vasopressin in response to patterned bursts of APs. We used trains of de-

Received Sept. 19, 1994; revised Nov. 28, 1994; accepted Dec. 5, 1994.

This work was supported by an NINCDS grant (M.C.N.) and a Medical Research Council of Canada fellowship (E.P.S.). We thank Dr. Kathrin Engisch for critically reading the manuscript.

Correspondence should be addressed to Martha C. Nowycky at the above address.

[a]Present address: Glaxo Institute for Molecular Biology, 14 ch. des Aulx, 228 Plan-les-Ouates, Geneva, Switzerland.

polarizing pulses to mimic the physiological stimuli in which [Ca^{2+}] would increase transiently near the membrane during relatively brief APs and then decay due to subsequent buffering and diffusion in the intervals between APs. If exocytosis of LDCVs in nerve terminals has the same characteristics reported for chromaffin cells and melanotrophs, at least three predictions follow for a train of depolarizing stimuli: (1) during a train of depolarizations the rate of secretion should be greatest at the start of a train and then decline as the pool is depleted; (2) protocols that increase current amplitude should produce more secretion than increases in pulse duration since the former results in a higher elevation of submembrane [Ca^{2+}] (Sala and Hernadez-Cruz, 1990; Nowycky and Pinter, 1993); (3) a Ca^{2+} chelator with slow binding kinetics such as EGTA will be a relatively poor inhibitor of peptide secretion while BAPTA, which has ~100× faster forward binding kinetics, would have greater effect on secretion because it will lower submembrane [Ca^{2+}] more effectively (Adler et al., 1991; Roberts, 1994).

"Whole-terminal" patch-clamp recordings of acutely isolated NHP terminals were used to measure changes in C_m triggered by Ca^{2+} influx through voltage-dependent Ca^{2+} channels (Neher and Marty, 1982; Joshi and Fernandez, 1988; Fidler and Fernandez, 1989). Exocytosis of LDCVs in these nerve terminals has a triphasic relationship to Ca^{2+} entry and is very sensitive to both EGTA and BAPTA. We propose that at rest there are no "docked" or "readily releasable" vesicles in NHP terminals. Instead, at least two kinetically distinct Ca^{2+} sensors are involved in exocytosis of LDCVs once stimulation is initiated. The first step is purely preparatory, while the second triggers release. This is followed by depression or fatigue. Our findings correlate well with data obtained with intact neurohypophyses (Dutton and Dyball, 1979; Cazalis et al., 1985; Leng, 1988). The lack of applicability of the model developed for secretion of LDCV in chromaffin cells and melanotrophs to NHP terminals indicates that stimulus–secretion coupling kinetics may be heterologous even for a single class of vesicles.

Some of these results have been presented previously in abstract form (Seward et al., 1992, 1993).

Materials and Methods

NHP terminal preparation. Nerve terminals were isolated from adult male rat neurohypophyses using modifications of previously described methods (Cazalis et al., 1987a,b). In brief, rats were anesthetized with CO_2 and decapitated, and the posterior pituitary was dissected from the anterior and intermediate pituitary in a low-Ca^{2+} solution consisting of (mM) NaCl, 145; KCl, 5; $MgCl_2$, 1; EGTA, 2; $CaCl_2$, 1.9; and HEPES, 10; glucose, 10; pH 7.2 with NaOH. Isolated neurohypophyses were then minced and homogenized in a sucrose solution consisting of (mM) sucrose, 270; EGTA, 0.01; and HEPES, 10; pH 7.2 with KOH. The resulting suspension of terminals was plated on poly-L-lysine (Sigma)–coated coverslips and left to adhere for 30 min. Ca^{2+} was gradually reintroduced to attached terminals by dilution of the sucrose solution with extracellular solution consisting of (mM) NaCl, 145; KCl, 5; $MgCl_2$, 1; $CaCl_2$, 2.5; HEPES, 10; and glucose, 10; pH 7.2 with NaOH. Terminals were then either transferred to the recording chamber or placed in DMEM medium (GIBCO) supplemented with 5% fetal bovine serum (GIBCO) and stored in a 37°C incubator where they remained viable for up to 10 hr.

Electrophysiological recordings. Whole-terminal membrane current was recorded with an EPC-7 patch-clamp amplifier. Secretion was monitored on line with a computer based capacitance detection technique. To measure changes in C_m, a 15 mV rms, 1.2 kHz sine wave was added to the holding potential of −90 mV through the V-command input of the amplifier, as described previously (Lim et al., 1990). The resulting current output of the amplifier was passed through a 12 bit A/D converter, filtered at 3 kHz, and analyzed at two orthogonal phase angles, using PC-based software (Joshi and Fernandez, 1988). The correct phase angle for the phase-sensitive detector was located automatically by a 500 kΩ resistor in series with ground that was switched in and out under computer control (Fidler and Fernandez, 1989). Each data point represents the average of 10 sinusoidal cycles and was collected with a temporal resolution of 14–18 msec. C_m trace calibration was obtained by temporary displacement of the C_{slow} compensation network of the amplifier by 100 fF. Exocytosis was triggered by interrupting the sinusoid and applying trains of depolarizing pulses of variable voltage, duration, and frequency. The potential was returned to the holding potential of −90 mV after each pulse and the sinusoid restarted after a lag of ~50 msec. Thus, the first C_m point measured after application of each voltage step was calculated at ~68 msec after the end of the voltage step.

Terminals were easily identified from contaminating cells by their phase-bright, smooth appearance, lack of nucleus and high content of dark vesicles and by their neuronal-like, large, rapidly inactivating, TTX-sensitive sodium currents. In early experiments, TTX was omitted from the extracellular solution to aid in identification of the terminals.

Isolated terminals were patch-clamped with 5–10 MΩ electrodes coated with Sylgard (Corning). The internal solution consisted of (mM), Cs-D-glutamate, 115; HEPES, 40; $MgCl_2$, 1; CsCl, 10; Mg-ATP, 2.5; and EGTA (0.1–0.5) or BAPTA (0.1–1) as indicated in the text; pH 7.2 with CsOH. For solutions with high-Ca^{2+} buffer concentrations, EGTA (10 mM), and EGTA or BAPTA (3 mM), the concentration of Cs-D-glutamate was lowered to 98 and 112 mM, respectively. The extracellular solution was similar to that used to dilute the sucrose solution in terminal preparation, except $CaCl_2$ was increased to 10 mM and in most experiments 1 μM TTX was added.

Data analysis. The total change in C_m (ΔC_m) triggered by each voltage pulse of a train was determined off line as the sum of two components. (1) Changes in C_m occurring during a voltage pulse were measured by averaging four C_m points immediately before application of the pulse and subtracting this value from the average of the first four C_m points acquired immediately following the voltage pulse. (2) Drifts in C_m occurring after a pulse were assessed by taking the average of four C_m points at the beginning of the interpulse interval and subtracting from the average of four C_m points taken immediately before the next voltage pulse. For the last pulse of a train, the final four points were taken after an interval equivalent to the interpulse duration. ΔC_m is defined as the sum of C_m changes occurring during and after a single pulse. The total change in C_m resulting from a train of depolarizations was calculated as the sum of ΔC_m values for all pulses in the train, except where these are specifically segregated into stimulus "jumps" and poststimulus "drifts." In some terminals, each pulse was followed by a prominent downward drift in C_m, often exceeding any increase in C_m that occurred during the pulse. Since we cannot be certain whether the downward drifts are due to rapid endocytosis or some other non-exocytotic-related events (see Horrigan and Bookman, 1993) and do not know the extent of interference with estimates of exocytosis, these terminals have been excluded from analysis.

The Ca^{2+} ion influx per pulse was determined by integration of the recorded inward current. All currents were digitally leak subtracted. Leak currents were obtained at the beginning of each train by averaging and scaling currents recorded in response to 16 voltage steps to −110 mV from the holding potential of −90 mV. Limits for integration were set at the beginning and end of the Ca^{2+} current. Tail currents were excluded from the integration since they appear to be contaminated by a Ca^{2+}-activated outward current, as described in the text. In early experiments, where Na^+ currents were not blocked by TTX, the left limit was set at a point where this current appeared to be fully inactivated (~3 msec into the pulse).

"Thresholds" were estimated by extrapolating back to baseline (0–10 fF, depending on noise) a line fit by eye to the rising phase of plots of cumulative C_m versus cumulative integrated Ca^{2+} entry. Of the experiments presented here, certain traces were straight forward such as trace 2 in Figure 1. Other traces were more problematic, such as Figure 2*B*. A few traces were considered to be too difficult and were not included.

Results

Exocytosis begins with a delay that depends on the time integral of Ca^{2+} current

Terminals were stimulated with trains of depolarizing pulses to simulate the pulsatile Ca^{2+} entry that is expected during a burst

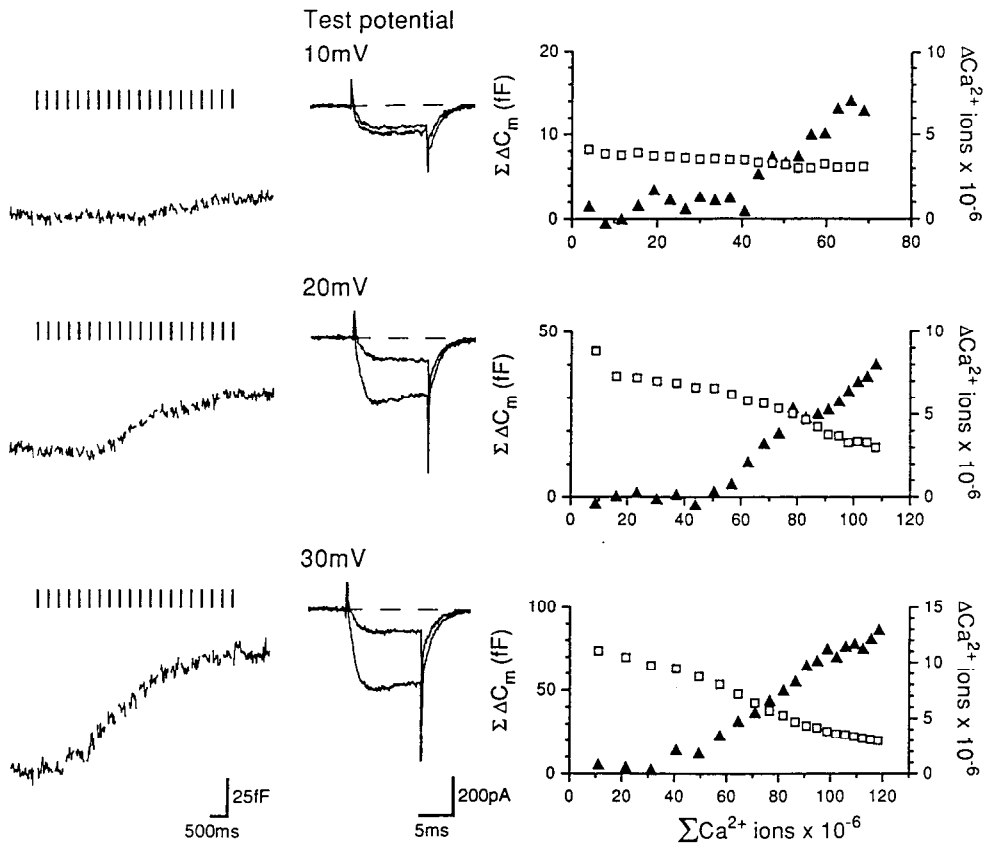

Figure 1. Trains of brief depolarizing voltage pulses trigger increases in NHP terminal membrane capacitance after a delay. *Left*, Changes in C_m recorded in a single NHP terminal in response to three stimulating trains of 20 pulses, 10 msec duration, from a holding potential (HP) of −90 mV to the test potentials (TP) indicated. *Gaps* in each trace (not drawn to scale) and the *vertical bars* above indicate depolarizing pulses. The interpulse interval was 200 msec and trains were separated by ~3 min. Stimulation with 20 pulses to 0 mV failed to elicit any increase in C_m in this terminal (data not shown). *Center*, Superimposed, leak-subtracted Ca^{2+} currents recorded during the first and last pulse of each corresponding train. The peak amplitude of the first Ca^{2+} current per train increases as the test potential is increased from +10 to +30 mV. Only influx during the test pulse was integrated, since the "tail" current is contaminated with a Ca^{2+}-activated nonspecific cation current. The approximate contribution of Ca^{2+} influx during repolarization can be appreciated by comparing the small difference in the two tail currents at +30 mV, which corresponds to the inactivation of ~75% of Ca^{2+} channels (unpublished observations). *Right*, The relationship between Ca^{2+} influx and exocytosis for each train is illustrated by plotting the cumulative increase in C_m (*left ordinate, filled triangles*) against the cumulative Ca^{2+} ion influx (*abscissa*). The Ca^{2+} ion influx per pulse was determined from the time integral and is plotted as a function of cumulative Ca^{2+} ion influx on the *right ordinate* (*open squares*). Ca^{2+} buffer: 0.5 mM BAPTA; terminal B16.

of action potentials. Recording conditions were designed to isolate voltage-activated Ca^{2+} currents (Lemos and Nowycky, 1989); contaminating outward K^+ currents were blocked by inclusion of Cs^+ in the pipette solution, and inward Na^+ currents were blocked by external TTX. Two parameters were varied to probe the relationship between Ca^{2+} influx and secretion: (1) the amplitude of the evoked Ca^{2+} current was varied by changing the test pulse potential, while pulse duration was constant, and (2) the time course of Ca^{2+} influx was varied by changing pulse duration, while pulse potential was constant.

The effect of varying Ca^{2+} flux (i.e., current amplitude) on stimulus-evoked secretion is shown in Figure 1. The amount of Ca^{2+} entering the terminal during a train was manipulated by depolarizing to progressively more positive test potentials, with the maximum flux occurring at +30 mV, the peak of the current–voltage relationship for Ca^{2+} currents in NHP terminals with intracellular Cs-glutamate (Lim et al., 1990). The increases in whole-terminal C_m measured in response to a series of such trains are shown in Figure 1 (left), with the Ca^{2+} currents recorded during the first and last voltage step of each train illustrated in Figure 1 (middle). The amplitude of the evoked Ca^{2+} currents decreased progressively during a train due to the cumulative effects of voltage-dependent and Ca^{2+}-dependent channel inactivation (Figure 1, right, open squares). At the most negative potential shown (+10 mV), where the probability of channel opening is low and consequently Ca^{2+} currents are relatively small, there is a long delay before any increases in C_m are observed. The first C_m jump occurred on the 11th pulse, corresponding to a delay of >2 sec. Increasing the amplitude of the Ca^{2+} current and therefore the Ca^{2+} flux shortened this delay to ~0.6 sec for the largest currents. To quantify the Ca^{2+} influx required for exocytosis, the time integrals of the evoked Ca^{2+} currents were calculated. The cumulative change in C_m is plotted for each pulse as a function of the cumulative Ca^{2+} entry (Fig. 1, right). In all three trains, ~40–50 × 10^6 Ca^{2+} ions entered the terminal before C_m began to increase. The delay in the onset of exocytosis depended on the number of pulses required for this "threshold" number of Ca^{2+} ions to enter. Similar results were obtained in six terminals.

If the amount of Ca^{2+} influx was varied by prolonging pulse duration at a constant test potential, the results were essentially identical (data not shown). C_m increases were observed with a

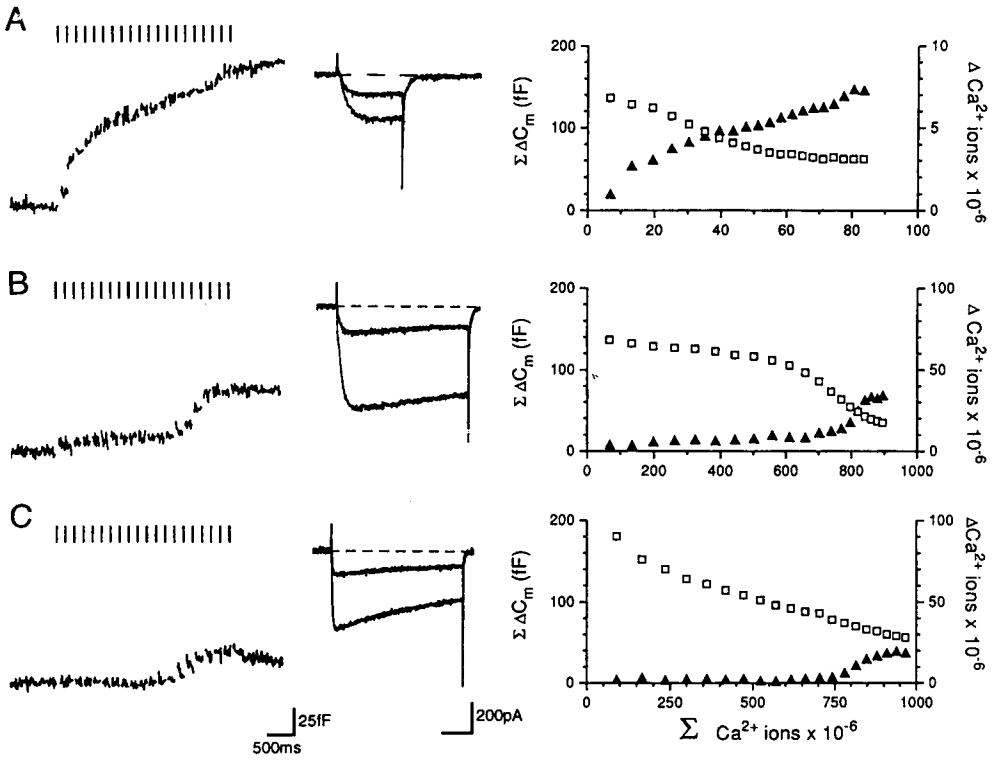

Figure 2. [EGTA]$_i$ modulates the amount of Ca^{2+} needed to initiate exocytosis. *A*, Data from a terminal dialyzed with 0.1 mM EGTA. Format is the same as in Figure 1. Pulses are of 10 msec duration to TP +20 mV. Terminal E0131. *B*, Data from another terminal (E0310), dialyzed with 3.0 mM EGTA and stimulated with 20 pulses, 40 msec, TP +20 mV. *C*, Data illustrated from a third terminal (E1001) with 10 mM EGTA in the pipette and stimulated by a train of 20 pulses, 80 msec, Tp +20 mV. Only 6 of 19 terminals had Ca^{2+} currents sufficiently large to elicit any secretion in 10 mM EGTA. For current traces, time calibration is 5 msec for *A*, 10 msec for *B*, and 20 msec for *C*.

delay that depended upon the cumulative Ca^{2+} ion influx. These results contrast to what would be predicted from the "microdomain" model of release (Simon and Llinas, 1985). Similar amplitude currents should be more effective at more negative potentials where the driving force on Ca^{2+} ions is larger. It also does not correspond to overlapping microdomains (Zucker and Fogelson, 1986; Roberts, 1994), since the largest C_m jumps should occur with the first pulse of a train when the current is largest and the greatest number of channels are open. For equivalent total Ca^{2+} entry, increased current amplitude should produce higher local $[Ca^{2+}]_i$ due to domain overlap than prolonged duration, which allows time for diffusion and buffering. In contrast to these expectations, changes in current amplitude or duration appear equally effective in initiating secretion and C_m increases are not strictly associated with the earliest pulses in the train, but instead appear to depend on achievement of a "threshold" accumulation of Ca^{2+} entry.

Low concentrations of EGTA and BAPTA influence the "threshold"

Our standard pipette solution contained 0.5 mM Ca^{2+} chelator. In the next set of experiments we varied the concentration and species of Ca^{2+} chelator. In contrast to the results at fast synapses (Adler et al., 1991), we found that even very low concentrations of EGTA had pronounced effects on stimulus–secretion coupling.

In Figure 2*A–C*, representative C_m traces are shown from three terminals recorded with 0.1, 3, and 10 mM EGTA in the patch pipette. In 0.1 mM EGTA, C_m increases often began with the first pulse, in response to a relatively modest Ca^{2+} current (Fig. 3*A*). In this example, enough Ca^{2+} entered the terminal during the first pulse (7×10^6 ions) to elicit a jump of 18 fF in C_m. Raising EGTA to 3 mM greatly increased the amount of Ca^{2+} needed to elicit secretion. Despite an ~10-fold increase in both the Ca^{2+} influx/pulse and cumulative Ca^{2+} entry (compare Fig. 2*A,B*), the total secretion elicited by the train is less (61 vs 144 fF). The threshold for secretion was estimated to be $\sim 700 \times 10^6$ ions in this terminal. The average value for 3.0 mM EGTA is $420 \pm 60 \times 10^6$ ions ($\pm$SEM, $n = 8$).

Inclusion of 10 mM EGTA completely suppressed C_m increases in the majority of terminals (13 of 19). If Ca^{2+} currents were unusually large (Fig. 2*C*), some increases were observed. The total secretion elicited by the train with 10 mM EGTA is attenuated compared with that observed with 3 mM EGTA (36 vs 61 fF) despite similar cumulative Ca^{2+} influx (967 vs 896×10^6 ions, respectively). The threshold for secretion in this experiment was estimated to be 720×10^6 Ca^{2+} ions. Thus, increasing $[EGTA]_i$ not only increased the threshold but also attenuated or abolished postthreshold secretion.

We also examined the effect of several concentrations of a second Ca^{2+} chelator, BAPTA. The Ca^{2+} affinities of EGTA and BAPTA are nearly identical (120–190 nM for EGTA vs 190 nM for BAPTA, calculated from Martell and Smith, 1974; Tsien, 1980); however their on-rates for Ca^{2+} binding differ by at least 2 orders of magnitude (Tsien, 1980). The difference in binding rate constant is responsible for the much greater efficacy of BAPTA over EGTA at the squid giant synapse (Adler et al., 1991).

Three representative traces obtained in 0.1, 1, and 3 mM BAPTA and their associated Ca^{2+} currents are shown in Figure 3. As for EGTA C_m increases may begin on the first or second pulse in 0.1 mM BAPTA. In the example illustrated in Figure 3*A*, a C_m increase was elicited by the first pulse after entry of 6×10^6 ions. C_m increases continued as a series of small steps, which in this experiment produced a cumulative increase of ~80 fF. In 1.0 mM BAPTA (Fig. 3*B*), C_m increases begin after the cumulative entry of $\sim 60 \times 10^6$ Ca^{2+} ions.

Only 1 of 15 terminals tested with 3 mM BAPTA in the pipette showed any C_m increases, even if cumulative Ca^{2+} entry exceeded 500×10^6 Ca^{2+} ions ($n = 6$). In contrast, of 19 terminals

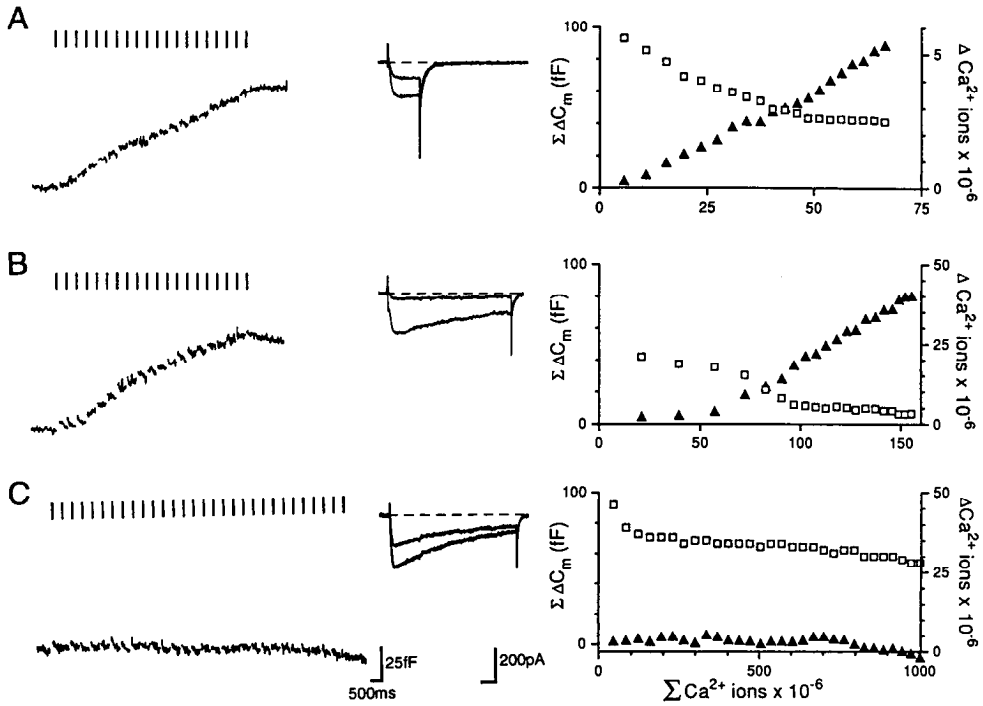

Figure 3. Effects of [BAPTA]$_i$ on threshold and secretion. *A*, C_m increases elicited by a train of 20 pulses, 10 msec, TP +20 mV with 0.1 mM [BAPTA]$_i$ are shown in the same format as Figures 1 and 2. Terminal B0101. *B*, Data from another terminal with 1 mM [BAPTA]$_i$, stimulated with a train of 20 pulses, 40 msec, TP +20 mV. Terminal B130. *C*, Data from a terminal dialyzed with 3 mM [BAPTA]$_i$ and stimulated with a train of 30 pulses, 80 msec, TP +20 mV. Terminal B0304. For current traces, time calibration is 5 msec for *A*, 10 msec for *B*, and 20 msec for *C*.

tested with 3 mM EGTA, 67% of terminals with similar Ca^{2+} influx showed C_m increases (n = 12). In Figure 3*C*, we show a flat C_m trace to illustrate the effectiveness of 3 mM BAPTA in suppressing C_m responses to large Ca^{2+} influx . Note that this concentration of BAPTA was also effective in minimizing Ca^{2+} current inactivation during the train.

In the experiments illustrated by Figures 1–3, depolarizing pulses were selected to be close to the minimum necessary to elicit C_m increases. For these protocols, there was a relatively clear amount of initial cumulative Ca^{2+} influx that did not elicit C_m increases. We used this as our operative definition of "Ca^{2+} threshold." The combined results from 48 terminals for both EGTA and BAPTA are summarized in Figure 4. The effect of EGTA concentration on threshold is shown over a 30-fold range (0.1–3.0 mM). The effect of BAPTA is very similar to that of EGTA, with no significant differences. The only deviation occurs at 3.0 mM BAPTA, which totally inhibited C_m increases, as discussed above.

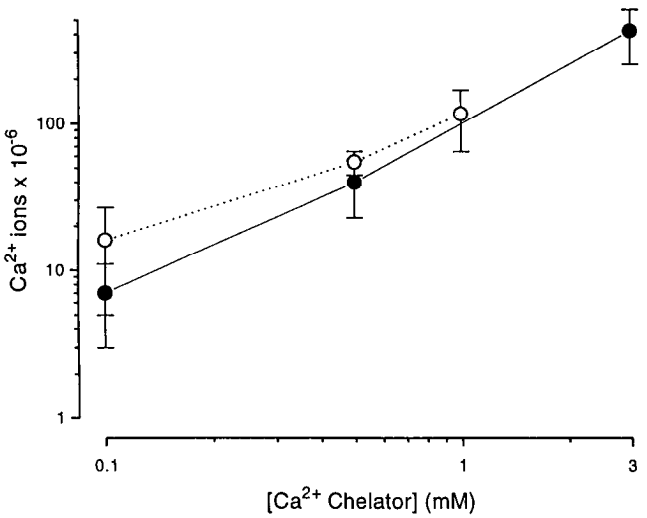

Figure 4. EGTA and BAPTA have similar potencies in modulating threshold. Data plotted are from 48 terminals and shows results from 69 determinations of threshold using various stimulation protocols. Values represent the mean number of Ca^{2+} ions (±SEM) required to initiate exocytosis, that is, "threshold," with different concentrations of EGTA (*filled circles*) or BAPTA (*open circles*) in the recording electrode. Thresholds were estimated as described in Materials and Methods. (In four of six terminals that had secretory response in 10 mM [EGTA]$_i$, ΔC_m were too small to allow good estimates of the threshold; consequently, this chelator concentration is not included.)

The secretory threshold can be reached during a single depolarizing pulse

The experiments described thus far used depolarizing pulses that were adjusted for minimal Ca^{2+} entry/pulse to simulate AP activity and clearly illustrate the threshold phenomenon. From here on we describe the results of pulse protocols that elicited larger amounts of Ca^{2+} influx during the first pulse. This was accomplished either by increasing pulse duration, or fortuitously, when an unusually large Ca^{2+} current was encountered. Data plotted in Figure 5, *A* and *B*, are from 94 terminals with either 0.1 mM or 0.5 mM EGTA, respectively, and show the amplitude of the first C_m step of a train plotted as a function of Ca^{2+} flux and pulse duration. Note that "flux" is an average estimate of true flux during a pulse since it was calculated as the time integrated Ca^{2+} current divided by the pulse duration without correcting for the time course of Ca^{2+} current activation or inactivation.

Large C_m jumps (20–70 fF) occurred in response to single depolarizations, clearly demonstrating that the secretory phase can be reached during a single pulse. The curve superimposed on the plots represents the threshold values for the appropriate chelator concentrations obtained from Figure 4. Almost all of the larger jumps occur to the right of this line; that is, even during a single pulse, large jumps are elicited only when the threshold value is exceeded. Otherwise, there is no obvious relationship between ΔC_m amplitude during a single depolarization and either pulse duration or Ca^{2+} flux.

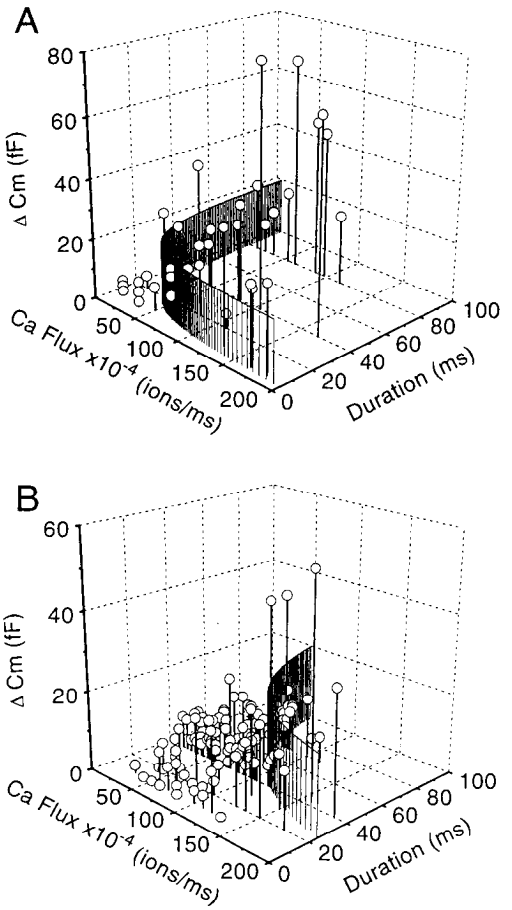

Figure 5. A single depolarizing pulse with Ca^{2+} entry above "threshold" can evoke large C_m jumps. ΔC_m for the first pulse in a train is plotted versus pulse duration and versus average Ca^{2+} flux in 0.1 (*A*) versus 0.5 mM (*B*) $[EGTA]_i$. The average number of Ca^{2+} ions required to initiate exocytosis ("threshold," determined in Fig. 4) is drawn as a ribbon. The height of the ribbon is 20 fF and was arbitrarily selected. *A*, In 0.1 mM $[EGTA]_i$ the "threshold" is 7×10^6 Ca^{2+} ions. *B*, In 0.5 mM $[EGTA]_i$ the "threshold" is 48×10^6 Ca^{2+} ions.

The data in Figure 5 include most of the largest individual C_m jumps we have observed in all of our experiments. The largest are almost all <60 fF, or about 20–30 vesicles. One limiting factor is the refractoriness of the secretory machinery that was previously termed secretory fatigue or depression (Lim et al., 1990). Additionally, some of the variability in ΔC_m amplitude is due to the stochastic noise inherent in any system with few events.

Characteristics of postthreshold Ca^{2+}–C_m coupling

Ca^{2+} chelators continue to exert an effect on secretion even after threshold is reached, suggesting they are not saturated at threshold. For the same total Ca^{2+} load, C_m responses are smaller in higher $[EGTA]_i$ (Fig. 6*A*, compare top two traces; note twofold difference in scale). The effects of equimolar BAPTA and EGTA on the C_m response for a comparable Ca^{2+} load are illustrated in the lower two traces of Figure 6*A*. In contrast to the results obtained on threshold, in the secretory phase BAPTA is more potent than EGTA. Summary data comparing 0.1 and 0.5 mM EGTA and 0.5 mM BAPTA are shown in Figure 6*B*. As expected, there is much more secretion at the lowest EGTA concentration, particularly at the highest Ca^{2+} loads. Maximal responses in 0.5 mM EGTA were achieved with much smaller Ca^{2+} loads than required for equimolar BAPTA. Additionally, all secretory responses were blocked in 3 mM BAPTA, but not in 3 mM EGTA (data not shown). These results suggest that above threshold, the faster on-rate kinetics of BAPTA make it more effective than EGTA in competing for Ca^{2+} with at least one of the "Ca^{2+} receptors" for secretion.

In the secretory phase, C_m increases were still dependent on the magnitude of Ca^{2+} influx. We tested the ability of short pulses to elicit secretion in the middle of a train, at a time when the Ca^{2+} threshold was clearly exceeded. An example is illustrated in Figure 7. In the control trace (Fig. 7*a*), a large C_m jump occurred in response to the second pulse. When the second pulse was decreased from 70 to 25 (Fig. 7*b*) or 12 (Fig. 7*c*) msec, the diminished Ca^{2+} entry elicited progressively smaller C_m jumps. Note that the total amount of secretion for each train was very similar.

A characteristic feature of depolarization evoked C_m increases in these terminals is its tight coupling to periods of Ca^{2+} influx. Once threshold is reached, most increases in C_m tended to occur as clear jumps during a depolarization (Figs. 6*A*, 7*a–c*) with little upward drift between pulses (for an example of "drift," see Fig. 6*A*, middle trace, third pulse). We compared the fraction of total C_m response that occurred during the pulses versus the amount that occurred between pulses. With 0.5 mM $[EGTA]_i$, 79 ± 2% (n = 47) of the total C_m increase occurred during the depolarizations. Even under reduced buffering conditions with 0.1 mM $[EGTA]_i$, 80 ± 5% of the total C_m increase occurred during the depolarizations (n = 13). Since C_m did not increase significantly between pulses, the final step(s) of exocytosis must require elevated submembrane $[Ca^{2+}]$ that dissipates quickly at pulse termination.

Discussion

We have examined the relationship between Ca^{2+} influx and exocytosis in peptide-secreting NHP terminals. NHP terminals secrete in response to patterned bursts of APs. APs early in the burst have a 1 msec duration, but then broaden to a maximum of 3–5 msec (Bourque and Renaud, 1988). AP frequencies range from 60 Hz at the beginning of a burst to 1–5 Hz at the end. Mathematical modeling suggests that this will cause a complex pattern of pulsatile Ca^{2+} entry: transient elevation of $[Ca^{2+}]$ near the membrane during APs, followed by diffusion, uptake, and buffering between APs (Sala and Hernandez-Cruz, 1990; Nowycky and Pinter, 1993). Here we used trains of short depolarizations to simulate bursts of APs and investigate the parameters of Ca^{2+} influx–secretion coupling in NHP terminals.

Recent models for exocytosis in chromaffin cells and melanotrophs propose that the final step of Ca^{2+}–secretion coupling of LDCV has a high-order dependence on absolute levels of Ca^{2+} concentration. Surprisingly, in our experiments, none of the pulse paradigms that should produce higher submembrane $[Ca^{2+}]$ had a simple relationship, either linear or higher order, with secretion. Instead, over a wide range of protocols, and despite the complex dynamics of $[Ca^{2+}]$ near the membrane due to diffusion, buffering, and Ca^{2+} channel inactivation, we found that secretion in different terminals could be related to the cumulative integrals of Ca^{2+} current.

Summary of major features of Ca^{2+}–secretion coupling in NHP terminals

During trains, two states of responsiveness to Ca^{2+} are observed: an early phase, in which Ca^{2+} entry does not trigger C_m increases

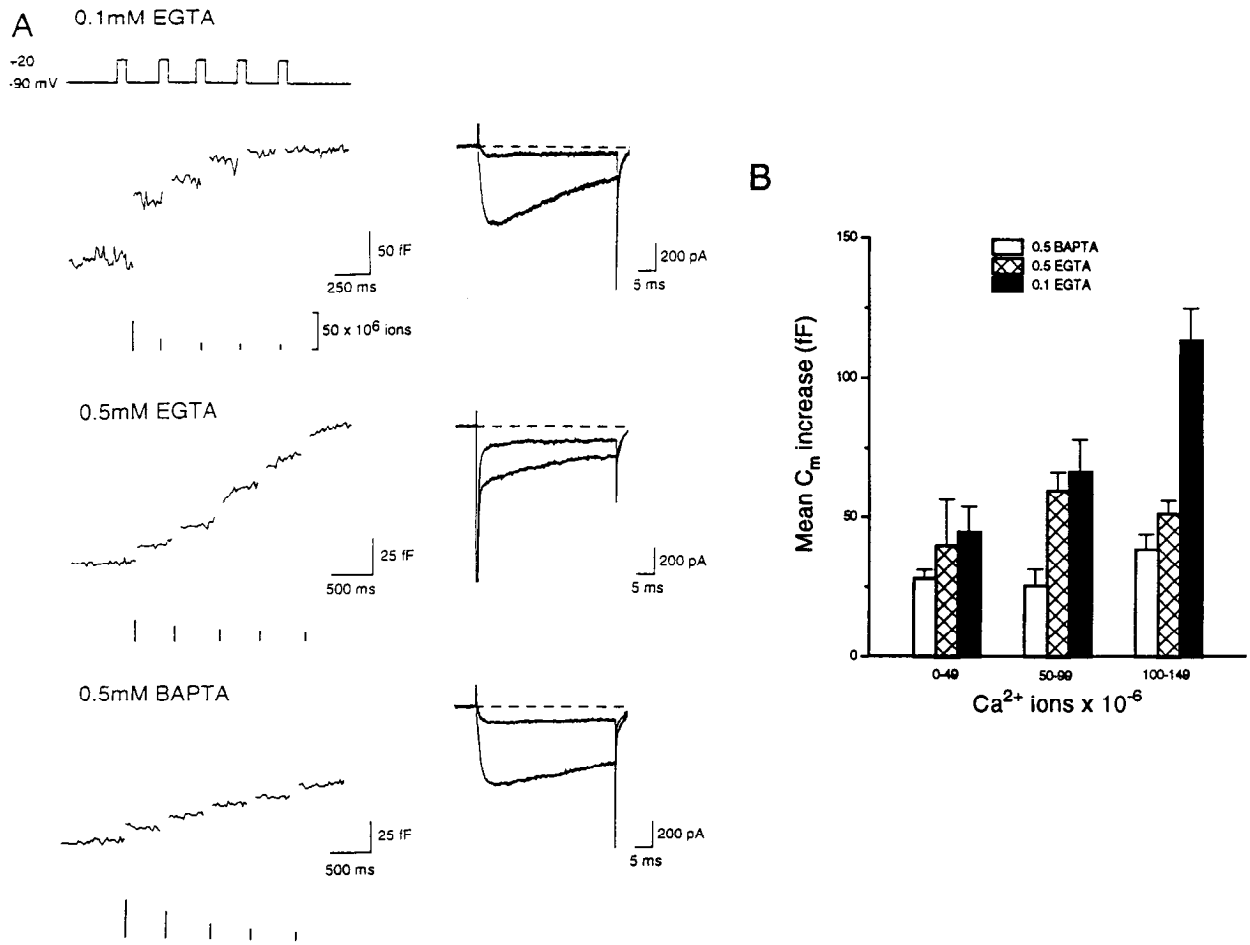

Figure 6. Effects of $[EGTA]_i$ and $[BAPTA]_i$ on the secretory phase. *A*, C_m responses in three terminals with different internal Ca^{2+} buffering conditions, as indicated. The pulse protocol used to stimulate the terminals (five pulses, 40 msec duration) is illustrated at the *top* and was chosen to evoke enough Ca^{2+} influx during the first pulse to reach threshold. *Bars* drawn below each C_m trace represent the integrated Ca^{2+} ion influx evoked per pulse. The first and last evoked currents are shown superimposed on the *right*. (The initial large, rapidly inactivating current in the 0.5 mM EGTA current traces is a TTX-sensitive Na^+ current.) With 0.1 mM $[EGTA]_i$, the rate of exocytosis is maximal during the first pulse (~778 fF/sec). With 0.5 mM $[EGTA]_i$ the total secretory response is smaller despite the larger total Ca^{2+} influx. With 0.5 mM $[BAPTA]_i$, all of C_m jumps are small and total secretion is diminished despite a somewhat larger total Ca^{2+} influx than in the example for 0.5 mM EGTA. The interpulse interval was 200 msec in the top train, and 400 msec in the lower two trains. We saw no secretory differences between these two pulse frequencies. Terminals E0117, A32, B1. *B*, Comparison of the total ΔC_m/train plotted against total Ca^{2+} influx with 0.1 mM and 0.5 mM $[EGTA]_i$ and 0.5 mM $[BAPTA]_i$. Bars are plotted within the appropriate bin. Error bars represent SEM. BAPTA is a more potent buffer than EGTA at low Ca^{2+} levels; 0.5 mM EGTA exerts a significant block of secretion compared to 0.1 mM EGTA.

("threshold" phase), and a subsequent phase, with diminished Ca^{2+} entry/pulse, which triggers C_m increases ("secretory" phase). After only a small number of vesicles are released, further Ca^{2+} influx does not produce C_m increases until after an appropriate rest period (Lim et al., 1990; Stuenkel and Nordmann, 1993; E. P. Seward, N. I. Chernevskaya, and M. C. Nowycky, unpublished observations, but see Figs. 6*A*, 7). The major features of the threshold and secretory phase include the following.

Threshold phase

(1) The threshold phase is defined as a period in which Ca^{2+} influx caused by depolarizing pulses does not produce significant C_m increases.

(2) The amount of Ca^{2+} entry necessary to reach threshold is determined by the concentration, but not the species, of exogenous Ca^{2+} chelator for EGTA versus BAPTA.

(3) The threshold amount of Ca^{2+} entry is remarkably independent of the pattern of Ca^{2+} influx and can be achieved by a single long depolarization (e.g., 80 msec in 0.1 or 0.5 mM chelator) or by a series of short pulses delivered over several seconds at ~4 Hz.

Secretory phase

(4) C_m jumps are coupled to periods of active Ca^{2+} influx, indicating that exocytosis occurs in response to elevated submembrane $[Ca^{2+}]$, which dissipates between pulses.

(5) BAPTA, a more rapidly binding Ca^{2+} chelator, diminishes the amount of secretion more effectively than equimolar concentrations of EGTA.

(6) The secretory response corresponds more to the integral of Ca^{2+} current rather than preferentially to increased current amplitude (higher submembrane $[Ca^{2+}]$) or duration (more sustained elevations of $[Ca^{2+}]$).

The threshold point is determined by exogenous chelator concentration

Since Ca^{2+} entry during the threshold phase does not trigger C_m increases, the threshold reflects either (1) insufficient Ca^{2+} levels

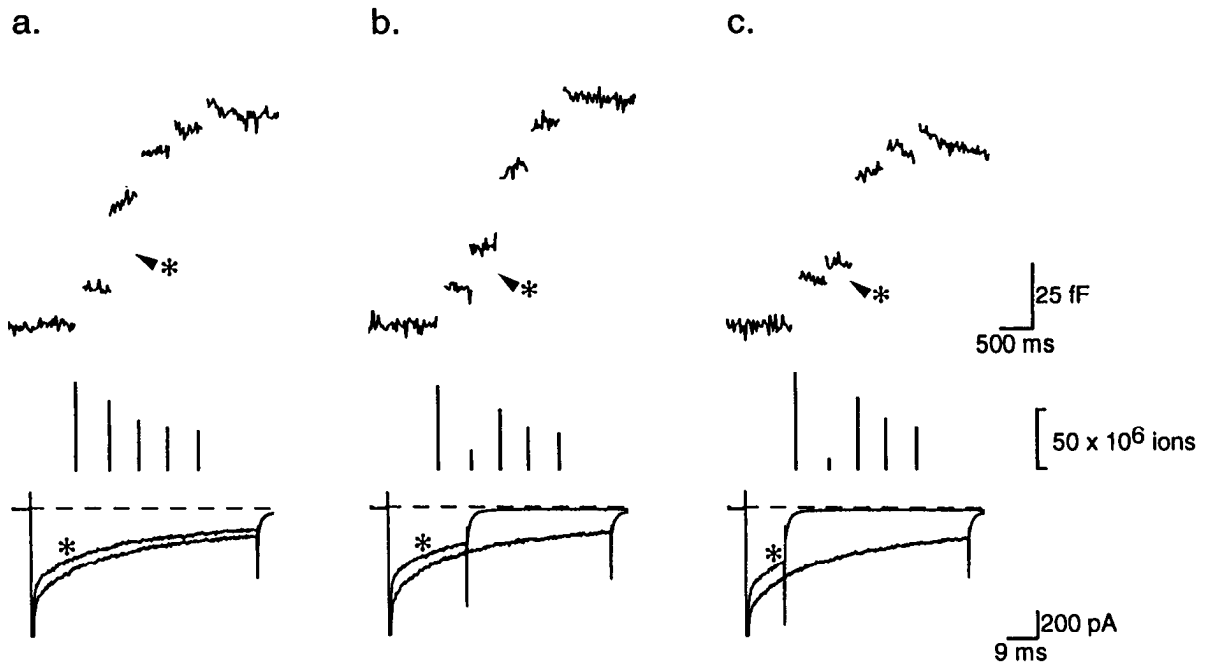

Figure 7. Exocytotic jumps are tightly coupled to active Ca^{2+} influx and require additional Ca^{2+} beyond threshold. *Top*, C_m traces recorded in a single terminal in response to trains of five pulses to +30 mV in which the duration of the second pulse (*) was varied. *Center*, *Vertical bars* represent the integrated Ca^{2+} ion influx evoked per pulse. *Bottom*, Superimposed first and second (*) currents evoked by the train. The initial, rapidly inactivating currents are TTX-sensitive Na^+ currents. *a*, "Control" trace in which all five pulses were of 70 msec duration. The second pulse evoked an increase of 38 fF/59 × 10^6 Ca^{2+} ions. *b*, The duration of the second pulse was decreased to 25 msec and evoked an increase of 19 fF/15 × 10^6 Ca^{2+} ions. *c*, Second pulse duration decreased further to 12 msec resulting in an increase of only 7 fF/8 × 10^6 Ca^{2+} ions. Ca^{2+} buffer: 0.5 mM EGTA; terminal A29.

in some critical space or (2) a Ca^{2+}-dependent "priming" step. It is not simply a time delay because while the threshold amount of Ca^{2+} is usually achieved over many seconds, it can also be reached by pulses as short as 5–10 msec with 0.1 mM EGTA.

The first explanation assumes that at rest, there is a vesicle population that requires Ca^{2+} binding to a single final receptor or class of receptors of low affinity (Heinemann et al., 1993; Thomas et al., 1993a). If this is correct and Ca^{2+} chelator concentration is a regulating factor, a simple explanation for the threshold phase is that submembrane $[Ca^{2+}]$ can increase to adequate levels for secretion only after chelator saturation. As discussed in the introductory remarks, this predicts that the threshold Ca^{2+} requirement should decrease with pulse protocols that produce higher submembrane $[Ca^{2+}]$.

Instead, the most striking and unexpected feature of the threshold is that it depends solely on the total amount of Ca^{2+} influx and concentration of exogenous Ca^{2+} chelator, but is independent of Ca^{2+} entry dynamics or binding kinetics of the chelator. For example, a slowly binding chelator such as EGTA should be easily overcome by larger-amplitude currents even when present in millimolar concentrations (Nowycky and Pinter, 1993, their Fig. 9). At equimolar concentrations, BAPTA should lower submembrane $[Ca^{2+}]$ more effectively than EGTA because its fast binding kinetics would trap and remove local $[Ca^{2+}]$ much more efficiently (Neher, 1986; Sala and Hernadez-Cruz, 1990; Adler et al., 1991; Nowycky and Pinter, 1993; Sullivan et al., 1993; Roberts, 1994). However, the buffers are equally effective in determining threshold.

Also, the chelators do not appear to be saturated at threshold, since they exert considerable effect on Ca^{2+}–secretion coupling during the secretory phase: (1) nearly complete block of C_m increases occurred with 3 mM BAPTA, but required ≥10 mM EGTA; (2) the total C_m increases/pulse train was greater in 0.5 mM EGTA than in equimolar BAPTA, although the threshold values were identical; (3) at higher concentrations of either buffer, progressively larger current amplitudes or durations were required to elicit any C_m increases; (4) finally, buffer saturation of chelators with dissociation constants of about 0.2 μM appears to be unachievable in NHP terminals because of powerful endogenous Ca^{2+} homeostatic mechanisms which maintain average Ca^{2+} at ≤500 nM (Stuenkel, 1993). At 500 nM, Ca^{2+} chelators will be unsaturated to the same percentage at different concentrations and therefore millimolar amounts of chelator will remain free at the higher concentrations used in these experiments.

Interpretations of the Ca^{2+} threshold

We postulate that the threshold phase reflects a Ca^{2+}-dependent priming step, rather than insufficient submembrane Ca^{2+}. Since the secretory phase is initiated after a fixed amount of Ca^{2+} influx governed by exogenous chelator concentration, the priming step may require distal or global elevation of $[Ca^{2+}]$. Alternatively, the secretory machinery of NHP terminals may respond to the recent history of Ca^{2+} influx.

A requirement for global elevation of $[Ca^{2+}]_i$ is supported by data from two groups who combined capacitance recordings with extensive fura-2 measurements of spatially averaged $[Ca^{2+}]_i$ in NHP terminals. Okano (1992) reported a threshold amount of 500–600 nM $[Ca^{2+}]_i$ that had to be exceeded for initiation of secretion. Lindau et al. (1992) obtained C_m increases > 30 fF only when $[Ca^{2+}]_i$ was >500–700 nM. In a separate set of experiments, Jackson et al. (1991) stimulated fura-2–loaded, intact NHP endings with trains of current pulses that mimicked pro-

tocols required for secretion. Average $[Ca^{2+}]_i$ changes paralleled the frequency dependence of secretion and achieved maximal levels of roughly threefold above baseline (i.e., ~300 nM). Thus, if global $[Ca^{2+}]$ increases are required these will be within ~300–600 nM $[Ca^{2+}]$. The upper limit follows in light of more recent work demonstrating that NHP terminals effectively clamp $[Ca^{2+}]_i$ to 500 nM irrespective of the Ca^{2+} load (Stuenkel, 1993).

Alternatively the priming step may respond to the recent history of Ca^{2+} influx rather than any absolute global elevations. This could be accomplished by a class of receptors that release Ca^{2+} very slowly after binding, or perhaps even require the cooperation of a cofactor or a phosphorylation–dephosphorylation step for Ca^{2+} dissociation. One supportive piece of evidence is that C_m increases can be obtained by a single relatively short pulse in 0.1 mM chelator, which may be too brief for global elevation of $[Ca^{2+}]_i$. Further experiments are necessary to resolve the mechanistic nature of the threshold phase.

Secretory phase

The relationship between Ca^{2+} influx and secretion during the second phase is difficult to quantify because of the limited amount of secretion per train that results in considerable stochastic variability between responses. Qualitatively, several characteristics distinguish the secretory phase from the threshold phase. The secretory phase is tied more directly to the elevated $[Ca^{2+}]$ near the membrane. This is manifested by (1) C_m increases occurring predominantly during periods of active Ca^{2+} influx, rather than between pulses, when Ca^{2+} gradients are dissipating; (2) the species of Ca^{2+} chelator is significant, since the more rapidly binding BAPTA is more effective in decreasing secretory responses during this phase than equimolar EGTA.

As in the threshold phase, the secretory response is correlated with the integral of Ca^{2+} current. We have not detected any process that responds as a high order function of $[Ca^{2+}]$ in NHP terminals, as has been reported for melanotrophs (Thomas et al., 1993a) and chromaffin cells (Augustine and Neher, 1992). The "facilitation" we observed in an earlier paper (Lim et al., 1990) is probably a consequence of reaching threshold on the first or second step (see Fig. 7).

Model for Ca^{2+}–secretion coupling in NHP terminals

The simplest model that explains our observations is that during a train of APs a minimum of two kinetically distinguishable Ca^{2+}-dependent receptors regulate secretion in NHP terminals. The first class of receptors does not regulate the fusion step directly, but it prepares vesicles for fusion in a step that must be accomplished before subsequent exocytotic steps can occur. In low buffering conditions, the threshold can be exceeded during the first pulse, indicating that threshold step is at least as fast as the maximal detected rate of membrane fusion (~1000 fF/s). During the intervals between trains (1–3 min duration) the system returns to basal conditions.

Comparison to Ca^{2+}-triggered secretion of LDCV in other systems

Recently, several studies have probed the relationship between Ca^{2+} and exocytosis of LDCVs by uniform elevation of Ca^{2+} via flash photolysis of DM-nitrophen in chromaffin cells (Neher and Zucker, 1993) and melanotrophs (Thomas et al., 1993a,b) or dialysis with elevated Ca^{2+} in the pipette (Augustine and Neher, 1992). In both systems, the authors concluded that a small pool of vesicles is ready to be released relatively rapidly by Ca^{2+} elevation although with a minimum delay that is severalfold longer than for SSVs. This pool is released by Ca^{2+} entry with a third-order or higher dependence on submembrane $[Ca^{2+}]$ at maximal rates of ~1000 fF/sec. Following depletion of the pool (which has a maximal size of about 400 − 600 fF in chromaffin cells and melanotrophs), the pool is refilled slowly in a Ca^{2+}-dependent manner with a maximal rate of about 45 fF/sec (Heinemann et al., 1993) or 26 fF/sec (Thomas et al., 1993a). Thus, the models postulated for chromaffin cells and melanotrophs differ both in the Ca^{2+} requirements of the final step and the requirement for passing through a threshold step that is reversible in the interval between trains of APs.

Studies on NHP terminals that support a threshold phase were reported above. Threshold phenomena or priming steps have been reported for other systems that secrete LDCVs. Secretion of LHRH from sympathetic neurons was examined by stimulating with AP trains of various frequencies combined with simultaneous imaging of $[Ca^{2+}]$ with fura-2 (Peng and Zucker, 1993). The authors conclude that the amount of secreted LHRH corresponded most closely to the integral of measured $[Ca^{2+}]_i$ above threshold. Insulin-secreting β-cells also have a requirement for threshold elevation of $[Ca^{2+}]$ to 0.5 μM (Ammala et al., 1993). Even in chromaffin cells, vesicles may not always be in a docked or release ready state. Priming steps that occur during a train of pulses have been invoked by us (Nowycky, 1992) and Artalejo et al. (1994). Thus, it is not clear whether the models of Neher's and Almers's laboratories are universally applicable to secretion of LDCVs, particularly when secretion is evoked through pulsatile Ca^{2+} entry. Further work is needed in all of these systems to dissect the various modes of secretion.

Physiological significance for secretion of LDCVs in NHP terminals

The choice of plotting secretion as a function of cumulative integrals of Ca^{2+} current was made empirically. This provided a surprising order to the complexity of pulsatile Ca^{2+} entry, buffering, and diffusion. Estimates of submembrane $[Ca^{2+}]$ alone were poorly related to the magnitude of secretion. The secretory response to the integral of Ca^{2+} entry indicates that, at a minimum, the secretory machinery responds to a product of $[Ca^{2+}]$ × time, rather than $[Ca^{2+}]$ alone.

The presence of two Ca^{2+}-dependent steps and absence of "docked" or "readily releasable" vesicles have important implications for stimulus–secretion coupling. Secretion of LDCVs from NHP terminals and many other excitable cells is triggered by bursts of APs (Leng, 1988). A system with at least two classes of Ca^{2+}-sensitive receptors, one of which requires global or distal elevation of Ca^{2+}, should respond to an AP burst with certain characteristic features. The first APs would contribute Ca^{2+} to elevate the levels globally and individual APs would not be able to elicit secretion. Once distal or global Ca^{2+} is elevated, subsequent APs would actually trigger release. Thus, the secretory machinery that corresponds to the threshold would not respond to random APs or trains that were inappropriately short. On the other hand, once the threshold was exceeded, APs late in an appropriate train would still efficiently elicit secretion, despite the diminishing Ca^{2+} entry that will result from N-type Ca^{2+} channel inactivation in these terminals (Lemos and Nowycky, 1989).

Many of the features predicted by this model fit with observations made with intact neural lobes. Short trains of APs do not elicit efficient vasopressin secretion (Shaw et al., 1984). AP

broadening is absolutely required, unlike at fast synapses (Bourque and Renaud, 1988). The presence of multiple Ca^{2+}-dependent steps suggests that the secretory machinery itself may be the target of modulation and various forms of synaptic plasticity, and will be regulated by the levels and properties of endogenous Ca^{2+} buffers.

References

Adler EM, Augustine GJ, Duffy SN, Charlton MP (1991) Alien intracellular calcium chelators attenuate neurotransmitter release at the squid giant synapse. J Neurosci 11:1496–1507.

Ammala C, Eliasson L, Bokvist K, Larsson O, Ashcroft FM, Rorsman P (1993) Exocytosis elicited by action potentials and voltage clamp calcium currents in individual mouse pancreatic B-cells. J Physiol 472:665–688.

Artalejo CR, Adams ME, Fox AP (1994) Three types of Ca^{2+} channel trigger secretion with different efficacies in chromaffin cells. Nature 367:72–76.

Augustine GJ, Neher E (1992) Calcium requirements for secretion in bovine chromaffin cells. J Physiol (Lond) 450:247–271.

Augustine GJ, Charlton MP, Smith SJ (1987) Calcium action in synaptic transmitter release. Annu Rev Neurosci 10:363–393.

Bourque CW, Renaud LP (1988) Activity dependence of action potential duration in neurosecretory cells. In: Pulsatility in neuroendocrine systems (Leng G, ed), pp 198–203. Boca Raton, FL: CRC.

Burgoyne RD (1991) Control of exocytosis in adrenal chromaffin cells. Biochim Biophys Acta 1071:174–202.

Cazalis M, Dayanithi G, Nordmann JJ (1985) The role of patterned burst and interburst interval on the excitation-coupling mechanism in the isolated rat neural lobe. J Physiol (Lond) 369:45–60.

Cazalis M, Dayanithi G, Nordmann JJ (1987a) Hormone release from isolated nerve endings of the rat neurohypophysis. J Physiol (Lond) 390:55–70.

Cazalis M, Dayanithi G, Nordmann JJ (1987b) Requirements for hormone release from permeabilized nerve endings isolated from the rat neurohypophysis. J Physiol (Lond) 390:71–91.

DeCamilli P, Jahn R (1990) Pathways to regulated exocytosis in neurons. Annu Rev Physiol 52:625–645.

Douglas WW, Poisner AM (1964a) Stimulus–secretion coupling in a neurosecretory organ: the role of calcium in the release of vasopressin from the neurohypophysis. J Physiol (Lond) 172:1–18.

Douglas WW, Poisner AM (1964b) Calcium movement in the neurohypophysis of the rat and its relation to the release of vasopressin. J Physiol (Lond) 172:19–30.

Dutton A, Dyball REJ (1979) Phasic firing enhances vasopressin release from the rat neurohypophysis. J Physiol (Lond) 290:433–440.

Fidler N, Fernandez JM (1989) Phase tracking: an improved phase detection technique for cell membrane capacitance measurements. Biophys J 56:1153–1162.

Heinemann C, von Ruden L, Chow RH, Neher E (1993) A two-step model of secretion control in neuroendocrine cells. Pfluegers Arch 424:105–112.

Horrigan, Bookman (1993) Biophys J 64:A101.

Jackson MB, Konnerth A, Augustine GJ (1991) Action potential broadening and frequency-dependent facilitation of calcium signals in pituitary nerve terminals. Proc Natl Acad Sci USA 88:380–384.

Joshi C, Fernandez JM (1988) Capacitance measurements. An analysis of the phase detector technique used to study exocytosis and endocytosis. Biophys J 53:885–892.

Lemos JR, Nowycky MC (1989) Two types of calcium channels coexist in peptide-releasing vertebrate nerve terminals. Neuron 2:1419–1426.

Leng G (1988) Pulsatility in neuroendocrine systems. Boca Raton, FL: CRC.

Lim NF, Nowycky MC, Bookman RJ (1990) Direct measurement of exocytosis and calcium currents in single vertebrate nerve terminals. Nature 344:449–451.

Lindau M, Stuenkel EL, Nordmann JJ (1992) Depolarization, intracellular calcium and exocytosis in single vertebrate nerve endings. Biophys J 61:19–30.

Martell AE, Smith RM (1974) Critical stability constants, Vol 1. New York: Plenum.

Morris JF, Pow DV (1988) Capturing and quantifying the exocytotic event. J Exp Biol 139:81–103.

Neher E (1986) Concentration profiles of calcium in the presence of a diffusible chelator. Exp Brain Res 14:80–96.

Neher E, Marty A (1982) Discrete changes of cell membrane capacitance observed under conditions of enhanced secretion in bovine adrenal chromaffin cells. Proc Natl Acad Sci USA 79:6712–6716.

Neher E, Zucker RS (1993) Multiple calcium-dependent processes related to secretion in bovine chromaffin cells. Neuron 10:21–30.

Nowycky MC (1992) Ca^{2+}-stimulated exocytosis in bovine chromaffin cells measured with the capacitance detection technique. Biophys J 61:A398.

Nowycky MC, Pinter MJ (1993) Time course of calcium and calcium-bound buffer transients in a model cell. Biophys J 64:77–91.

Okano K (1992) The relationship between cytosolic Ca^{2+} and exocytosis in single neurosecretosomes of rat neurohypophysis. Biophys J 61:A399.

Peng Y-y, Zucker RS (1993) Release of LHRH is linearly related to the time integral of presynaptic Ca^{2+} elevation above a threshold level in bullfrog sympathetic ganglia. Neuron 10:465–473.

Roberts WM (1994) Localization of calcium signals by a mobile calcium buffer in frog saccular hair cells. J Neurosci 14:3246–3262.

Sala F, Hernandez-Cruz A (1990) Calcium diffusion modeling in a spherical neuron. Relevance of buffering properties. Biophys J 57: 313–324.

Seward EP, Chernevskaya N, Nowycky MC (1992) Calcium entry, buffering and exocytosis in isolated peptidergic nerve terminals. Soc Neurosci Abstr 18:246.

Seward EP, Chernevskaya N, Nowycky MC (1993) Kinetic properties of stimulus-coupled exocytosis of large dense-cored vesicles from mammalian peptidergic nerve terminals. Biophys J 64:230a.

Shaw FD, Bicknell RJ, Dyball REJ (1984) Facilitation of vasopressin release from the neurohypophysis by application of electrical stimuli in bursts. Neuroendocrinology 348:601–618.

Simon SM, Llinas RR (1985) Compartmentalization of the submembrane calcium activity during calcium influx and its significance in transmitter release. Biophys J 48:485–.

Stuenkel EL (1993) Regulation of intracellular calcium in isolated secretory endings of the neurohypophysis. Soc Neurosci Abstr 19:1124.

Stuenkel EL, Nordmann JJ (1993) Intracellular calcium and vasopressin release of rat isolated neurohypophysial nerve endings. J Physiol (Lond) 468:335–355.

Sullivan KMC, Buss, WB, Wilson KL (1993) Calcium mobilization is required for nuclear vesicle fusion *in vitro*: implications for membrane traffic and IP3 receptor function. Cell 73:1411–1422.

Thomas P, Wong JG, Lee AK, Almers W (1993a) A low affinity Ca^{2+} receptor controls the final steps in peptide secretion from pituitary melanotrophs. Neuron 11:93–104.

Thomas P, Wong JG, Almers W (1993b) Millisecond studies of secretion in single rat pituitary cells stimulated by flash photolysis of caged Ca^{2+}. EMBO J 12:303–306.

Tsien RY (1980) New calcium indicators and buffers with high selectivity against magnesium and protons: design, synthesis and properties of prototype structures. Biochemistry 19 2396–2404.

Verhage M, McMahon HT, Ghijsen WEJM, Boomsma F, Scholten GWVM, Nicholls G (1991) Differential release of amino acids, neuropeptides and catecholamines from isolated nerve terminals. Neuron 6:517–524.

Zhu PC, Thureson-Klein A, Klein RL (1986) Exocytosis from large dense cored vesicles outside the active synaptic zones of terminals within the trigeminal subnucleus caudalis: a possible mechanism for neuropeptide release. Neuroscience 19:43–54.

Zucker RS, Fogelson AL (1986) Relationship between transmitter release and presynaptic calcium influx when calcium enters through discrete channels. Proc Natl Acad Sci USA 83:3032–3036.